Less safety for more efficiency: water relations and hydraulics of the invasive tree *Ailanthus altissima* (Mill.) Swingle compared with native *Fraxinus ornus* L.

Francesco Petruzzellis[1,3], Andrea Nardini[1,3], Tadeja Savi (iD) [1,2], Vanessa Tonet[1], Miris Castello[1] and Giovanni Bacaro[1]

[1]Dipartimento di Scienze della Vita, Università di Trieste, Via L. Giorgieri 10, 34127 Trieste, Italy; [2]University of Natural Resources and Life Sciences, Division of Viticulture and Pomology, Department of Crop Sciences, Konrad Lorenz Straße 24, A-3430 Tulln, Vienna, Austria; [3]Corresponding authors Andrea Nardini (nardini@units.it); Francesco Petruzzellis (francesco.petruzzellis@phd.units.it)

Invasion of natural habitats by alien trees is a threat to forest conservation. Our understanding of fundamental ecophysiological mechanisms promoting plant invasions is still limited, and hydraulic and water relation traits have been only seldom included in studies comparing native and invasive trees. We compared several leaf and wood functional and mechanistic traits in co-occurring *Ailanthus altissima* (Mill.) Swingle (Aa) and *Fraxinus ornus* L. (Fo). Aa is one of the most invasive woody species in Europe and North America, currently outcompeting several native trees including Fo. We aimed at quantifying inter-specific differences in terms of: (i) performance in resource use and acquisition; (ii) hydraulic efficiency and safety; (iii) carbon costs associated to leaf and wood construction; and (iv) plasticity of functional and mechanistic traits in response to light availability. Traits related to leaf and wood construction and drought resistance significantly differed between the two species. Fo sustained higher structural costs than Aa, but was more resistant to drought. The lower resistance to drought stress of Aa was counterbalanced by higher water transport efficiency, but possibly required mechanisms of resilience to drought-induced hydraulic damage. Larger phenotypic plasticity of Aa in response to light availability could also promote the invasive potential of the species.

Introduction

The invasion of natural habitats by alien plants is one of the most important threats to biodiversity conservation and ecosystem stability at regional and global scales (Pejchar and Mooney 2009, Pyšek et al. 2012). Invasion by alien trees is of particular concern because forests represent the largest carbon stock in terrestrial ecosystems and are also at the base of several biogeochemical and hydrological processes of fundamental importance (Bonan 2008). Hence, alterations in tree species' composition and abundance following invasion by alien trees is predicted to produce large and possibly irreversible impacts (Moser et al. 2009). This is especially worrying in the context of ongoing climate change, leading to higher frequency and intensity of droughts that are apparently increasing the dieback and mortality rates of forest trees (Hember et al. 2017, Neumann et al. 2017). Invasion by alien trees and resulting competition for water might accelerate these processes (Cavaleri and Sack 2010, Schachtschneider and February 2013), increasing the risk of native forest decline in the coming decades.

Our understanding of the fundamental ecophysiological mechanisms promoting invasion by alien tree species is still limited. Studies comparing functional traits of species with different growth forms and biogeography have revealed consistent patterns in traits' differences between alien and native species

(van Kleunen et al. 2010). In particular, invasive trees have been frequently reported to display higher values for traits related to resource acquisition compared with native tree species. These traits include high photosynthetic capacity, high specific leaf area and extensive root systems, all leading to increased biomass production in invasive species (Stratton and Goldstein 2001, Lamarque et al. 2011, Zeballos et al. 2014, Luo et al. 2016). In fact, invasive and native species typically occupy opposite ends in the leaf economic spectrum (Wright et al. 2004, Zeballos et al. 2014, Funk et al. 2016). Phenotypic plasticity, defined as the ability of a genotype to express different phenotypes in different environments (Nicotra et al. 2010), has been also proposed as an important trait favouring the invasive potential of alien species (Luo et al. 2016, Oliveira et al. 2017). Richards et al. (2006) proposed that plasticity of functional traits may allow invasive species to better acclimate to different environmental conditions than natives, thus broadening their ecological spatial amplitude or extending the period of active photosynthesis and biomass production on a seasonal scale (Stratton and Goldstein 2001, Nardini et al. 2003, Caplan and Yeakley 2013, Luo et al. 2016).

Despite large efforts devoted to identify functional traits related to invasiveness of alien woody species, most studies dealing with this topic have focused on traits relatively easy to measure, but often without clear mechanistic linkages with plant physiological performance. As an example, specific leaf area is one of the most used parameters in trait-based ecology, although it actually represents a 'syndrome trait' resulting from the interaction of several different processes including mass-based light-saturated photosynthetic rate, leaf lifespan and nutrient concentration, all finally influencing the plant-level growth rate (Poorter et al. 2009). However, 'mechanistic' traits (sensu Brodribb 2017) clearly associated with physiological processes hold better promise to provide meaningful information on fitness and performance of invasive plants compared with native ones. Among these, traits related to plant water relations and hydraulics are very interesting for studies focused on invasive trees, because the efficiency of root-to-leaf water transport is one of the factors most closely correlated to leaf gas exchange rates, maximum net photosynthesis, competition for water and relative growth rates (Nardini et al. 1999, Nardini 2002, Tyree 2003, Brodribb 2009). On the other hand, hydraulic safety expressed in terms of critical water potential values inducing xylem embolism (Urli et al. 2013, Zhu et al. 2017) or cell turgor loss (Binks et al. 2016, Savi et al. 2017) is the most critical factor for tree resistance to drought and persistence under water-limited conditions (Nardini et al. 2014a). Most importantly, it has been suggested that a trade-off exists between tree hydraulic safety and efficiency (Nardini and Luglio 2014, Gleason et al. 2016), and this trade-off might be important to explain interaction and competition processes during the invasion process.

Hydraulic and water relation traits have been only seldom included in studies comparing native and invasive trees, and results are somehow contrasting. As an example, Crous et al. (2012) reported that the invasive *Acacia mearnsii* had higher resistance to xylem embolism, and hence tolerance to drought, compared with two native species in fynbos riparian ecotones. A similar finding was reported by Yazaki et al. (2010) showing that saplings of the invasive *Psidium cattleianum* were more resistant to xylem embolism than native *Trema orientalis*. Opposite findings were reported by Zeballos et al. (2014), showing that wood density of invasive tree species was on average lower than that of native trees. This would suggest higher vulnerability to xylem embolism in invasive trees, considering the frequently reported correlation between wood density and xylem resistance to embolism (Markestejn et al. 2011, Nardini et al. 2013, Barotto et al. 2018). By comparing five pairs of co-occurring native and invasive trees, Pratt and Black (2006) concluded that hydraulic traits do not explain alone the invasive nature of tree species, although in two out of the five pairs considered, the invasive species turned out to be more vulnerable to embolism than the native ones.

Ailanthus altissima (Mill.) Swingle (hereafter referred to as Aa) is one of the most invasive woody species in Europe and North America, where it was introduced for ornamental and economical purposes from East Asia (Sladonja et al. 2015). The genus *Ailanthus* belongs to the family of Simaroubaceae. Members of this family have a primarily pantropical distribution (Clayton et al. 2007). However, the genera *Leitneria*, *Castela*, *Holacantha*, *Ailanthus*, *Picrasma* and *Brucea* include subtropical and temperate members. Although *Ailanthus* has an extensive fossil record dating from the early Eocene across the entire Northern Hemisphere (Corbett and Manchester 2004), Aa is at present the only species of the family represented in Europe, where it is considered alien and invasive. In its invasive range, the species is common in urban or disturbed areas, but in the Mediterranean region it also occurs in some natural habitats with increasing negative impacts on native outcompeted species (Gómez-Aparicio and Canham 2008, Constan-Nava et al. 2010). In the area selected for this study (Classical Karst, NE-Italy), Aa is currently outcompeting the native tree *Fraxinus ornus* L. (hereafter referred to as Fo) in post-disturbance vegetation successions as well as in natural forest regeneration processes, where Fo acts as a pioneer tree well adapted to exploit warm, sunny and water-limited habitats (Kalapos and Csontos 2003, Chiatante et al. 2006, Gortan et al. 2009). Fo is a member of the Oleaceae. The genus is represented in Europe by other species like *Fraxinus excelsior* or *Fraxinus angustifolia*, but these have quite different ecological requirements as they generally occur in mature forests with higher water availability.

The distribution ranges of Aa and Fo in Europe are largely overlapping (Caudullo et al. 2017), and the two species show

similar ecological requirements and habitat preferences (http://forest.jrc.ec.europa.eu/european-atlas-of-forest-tree-species). Aa and Fo share several common features, including small-to-medium size, presence of compound leaves, high seed production, fast growth, insect pollination, winged fruits (samaras) dispersed by wind, and the tendency to colonize and spread in open habitats. By measuring several leaf and wood functional and mechanistic traits in co-occurring Aa and Fo, we specifically aimed at testing inter-specific differences in terms of: (i) performance in resource use and acquisition; (ii) hydraulic efficiency and safety; (iii) carbon costs associated to leaf and wood construction; and (iv) plasticity of functional and mechanistic traits in response to light availability.

Materials and methods

Study area

The study area was located near the village of Gropada (North-Eastern Italy, 45.667390N, 13.846307E) in the Classical Karst, a limestone plateau extending by ~500 km^2 and characterized by a sub-Mediterranean climate. Summers are warm (average temperature 24.2 °C) with a short dry period occurring in July, while winters are mild (average temperature 7.5 °C), although frost events are not rare. Mean annual rainfall averages 900 mm (data from ARPA-OSMER, http://www.osmer.fvg.it, reference period 1996–2016). The natural vegetation is dominated by deciduous thermophilous mixed oak woodland, which alternates with *Pinus nigra* J.F. Arnold subsp. *nigra* plantations.

Two sites, each with an extension of ~1500 m^2 and characterized by contrasting light conditions (hereafter, L = site with high light availability and S = shaded site) were selected in the study area. The L site was located in an open grassland area undergoing progressive encroachment, where Aa was dominating over the native Fo. Here, individuals of both species had heights ranging from 1.5 to 5 m. The S site was located within a nearby pinewood where the dominant species in the canopy was *P. nigra* with a mean plant height in the range of 10–15 m and several individuals of Aa and Fo were present in the understory, with average heights of 1–3 m. Air temperature (*T*, °C), relative humidity (RH, %) and incident photosynthetic photon flux density (PPFD, µmol m^{-2} s^{-1}) were measured in each site at the same dates and times selected for field physiological measurements, using a thermo-hygro-anemometer (model 45160, Extech Instruments, Nashua, NH, USA) and a portable light metre (model HD 9021, Delta OHM srl, Padova, Italy), respectively. Five individuals of Aa and five of Fo were randomly selected in each site, and the functional traits listed in Table 1 were measured. All field measurements and sample collection for laboratory analyses were performed during 10 sunny days between the end of June and early July 2016.

Table 1. List of functional and mechanistic traits with their respective abbreviation and unit measured in *A. altissima* and in *F. ornus*.

Functional trait	Abbreviation	Unit
Leaf conductance to water vapour	g_L	mmol m^{-2} s^{-1}
Leaf transpiration rate	E_L	mmol m^{-2} s^{-1}
Pre-dawn leaf water potential	Ψ_{pd}	MPa
Minimum leaf water potential	Ψ_{min}	MPa
Leaf osmotic potential at full turgor	π_O	MPa
Leaf water potential at turgor loss point	Ψ_{tlp}	MPa
Stem specific hydraulic conductivity	K_s	kg m^{-1} s^{-1} MPa^{-1}
Whole-plant hydraulic conductance	k_{plant}	mmol m^{-2} s^{-1} MPa^{-1}
Water potential at 50% loss of conductivity	Ψ_{50}	MPa
Safety margin	SM	MPa
Wood density	WD	g cm^{-3}
Wood capacitance	C_{wood}	kg MPa^{-1} m^{-3}
Leaf dry matter content	LDMC	mg g^{-1}
Specific leaf area	SLA	mm^2 mg^{-1}
Major vein length per unit area	VLA$_{maj}$	mm mm^{-2}
Minor vein length per unit area	VLA$_{min}$	mm mm^{-2}
Leaf C to N ratio	C:N	/
Leaf C content	C	%
Leaf N content	N	%
Leaf ^{13}C isotopic composition	$\delta^{13}C$	‰

Plant water status and gas exchange

Leaf conductance to water vapour (g_L), minimum leaf water potential (Ψ_{min}) and pre-dawn leaf water potential (Ψ_{pd}) were measured on two leaves per individual selected from the outer part of the canopy. Both g_L and Ψ_{min} were measured between 12:30 and 15:00 h, using a steady-state porometer (SC-1 Decagon Devices Inc., Pullman, WA, USA) and a pressure chamber (mod. 1505D, PMS Instrument Company, Albany, OR, USA), respectively. Ψ_{pd} was measured between 4:00 and 5:00 h. For Ψ_{pd} and Ψ_{min}, leaves were detached from branches, wrapped in cling film and put in plastic bags with a piece of wet paper inside. Samples were stored in cool bags until measurements in the laboratory within 1–2 h from collection.

Estimating leaf transpiration rate and whole-plant hydraulic conductance

Leaf transpiration rate (E_L) was calculated as:

$$E_L = (VPD/p_{atm}) \times g_L$$

where VPD is the leaf-to-air vapour pressure deficit (kPa), p_{atm} is the atmospheric pressure (kPa) and g_L is the leaf conductance to water vapour (mmol m^{-2} s^{-1}). The VPD is given by VPD = VP$_{leaf}$ − VP$_{air}$, where VP$_{leaf}$ is the saturated water vapour pressure in the sub-stomatal cavity and VP$_{air}$ is the partial pressure of water vapour in the air. VP$_{air}$ and VP$_{leaf}$ were calculated

as $VP_x = VP_O \times (1 - RH)$, where VP_O is the vapour pressure at saturation and RH is the relative humidity recorded at the time when g_L was measured (see above). Relative humidity was assumed to be 100% in the leaf interior spaces.

On the basis of E_L values as well as Ψ_{min} and Ψ_{pd} (taken as a proxy for soil water potential measurements), whole-plant hydraulic conductance (k_{plant}) was calculated as:

$$k_{plant} = E_L/(\Psi_{pd} - \Psi_{min})$$

Water relation parameters

Osmotic potential at full turgor (π_O) and water potential at turgor loss point (Ψ_{tlp}) were measured on five leaves from five individuals, sampled on the basis of a hierarchically stratified random design (Petruzzellis et al. 2017). Leaves were detached from branches, wrapped in cling film and put in plastic bags with a piece of wet paper inside to avoid dehydration. Samples were stored in cool bags until processing in the laboratory. Measurements were done according to Bartlett et al. (2012) with some modifications. Fresh leaf laminas were first rehydrated overnight and were then roughly crumbled and sealed in cling film. Then, they were immersed in liquid nitrogen for 2 min. Leaves (still sealed in cling film) were then carefully ground and stored in sealed plastic bottles at $-20\,°C$ until measurements, when samples were thawed at room temperature for 5 min while still sealed in cling film and in plastic bottles. Measurements of π_O were done with a dew point hygrometer (Model WP4, Decagon Devices Inc.). Measurements of π_O using the method described above could be influenced by sample dilution due to apoplastic water. To overcome this limitation, π_O were corrected for different leaf dry matter content (LDMC; see below) using the following equation (Petruzzellis et al. in preparation):

$$\pi_O = (0.5303 \times \pi_{WP4}) + (0.0019 \times LDMC) - 0.001306$$

Ψ_{tlp} was finally calculated as:

$$\Psi_{tlp} = (1.31 \times \pi_O) - 0.03$$

Leaf morpho-anatomical traits

Five leaves from five individuals in each site and for each species were sampled as described for water relation parameters and leaf morpho-anatomical traits were measured. Leaf dry matter content and specific leaf area were calculated as:

$$LDMC = Leaf\ dry\ weight/Leaf\ turgid\ weight$$

$$SLA = (Leaf\ area)/(Leaf\ dry\ weight)$$

Fresh leaves were first rehydrated overnight and leaf turgid weight was measured with an analytical balance. Leaves were scanned using a scanner, and leaf area was measured using the software ImageJ. Leaves were finally oven-dried for 48 h at 72 °C and leaf dry weight was measured.

The lengths of major and minor veins per unit surface area (VLA_{maj} and VLA_{min}, respectively) were measured as:

$$VLA = Vein\ Length/Leaf\ sample\ area$$

To measure VLA_{maj}, fresh leaves were scanned and the ratio between vein length and sample area were measured using PhenoVein software (Bühler et al. 2015). For VLA_{min}, fresh leaves were cleared in 1 M NaOH solution for 48–72 h at room temperature, replacing solution when it turned dark coloured. Then, small portion of leaves (1 cm^2) were cut and bleached in 5% NaClO for 1–2 min. Samples were treated in a sequence of ethanol solutions at increasing concentration (25%, 50%, 75% and 100%) and then immersed in an alcoholic solution of toluidine blue (3%) overnight. Finally, samples were processed in a series of ethanol solutions at decreasing concentration and microscopic slides were prepared. Images of small portions (~5 mm^2) of leaves were captured with an optical microscope at 4× magnification equipped with a digital camera and VLA_{min} was measured using PhenoVein software.

Nutrient concentration and stable isotopes analysis

Nitrogen content (N %), carbon content (C %), C:N ratio and carbon isotopic composition ($\delta^{13}C$) were measured on one dried pulverized leaf randomly sampled from each individual of each species in L and S sites. Leaves were sampled as described above, oven-dried and then pulverized in a mortar. Samples were analysed for C and N contents (% dry weight), and stable isotope ratios were assessed via elemental analyser/continuous flow isotope ratio mass spectrometry using a CHNOS Elemental Analyser (vario ISOTOPE cube, Elementar, Hanau, Germany) coupled with an IsoPrime 100 mass spectrometer (Isoprime Ltd, Cheadle, UK). All isotope analyses were conducted at the Centre for Stable Isotope Biogeochemistry at the University of California, Berkeley. Long-term external precision based on reference material 'NIST SMR 1577b' (bovine liver) is 0.10‰ and 0.15‰ for C and N isotope analyses, respectively.

Wood density, wood capacitance and hydraulic conductivity measurements

Wood density (WD) and wood capacitance (C_{wood}) were measured on 2-year-old segments from one stem per each individual (10 stems per species, 5 per each site).

Wood density was calculated as:

$$WD = Wood\ dry\ weight/Wood\ dry\ volume$$

Bark was removed from 3 cm long segments before oven-drying the samples at 70 °C for 24 h. Samples were then weighed, and their dry volume was measured using a water displacement method (Hughes 2005).

To measure wood capacitance (C_{wood}), 3 cm long segments were longitudinally split in two parts. Bark was removed, and samples were soaked in water overnight. Fresh volume was measured as described for WD. Sequential measurements of sample weight and water potential (using the WP4 hygrometer, see above) were performed during bench dehydration. Measurements were performed in the Ψ range between 0 and -2.0 MPa. C_{wood} was calculated as the slope of the cumulative water loss vs Ψ linear relationship, normalized by fresh volume (Savi et al. 2017).

To estimate the vulnerability of the study species to drought-induced embolism formation, vulnerability curves were measured with classical hydraulic techniques coupled with bench dehydration. Embolism-induced loss of stem hydraulic conductance was measured on stem segments sampled from 2-year-old branches, randomly collected from all individuals included in the study (see above). Stems were detached from branches and the cut section was immediately put in water. Additional cuts were made under water to remove any eventual embolism induced by the initial cutting (Trifilò et al. 2014, Beikircher and Mayr 2016) and stems were immediately transported to the laboratory, where they were rehydrated overnight. Stems were left dehydrating in the laboratory for a minimum of 1 h up to a maximum of 4 days. At different time intervals, two apical leaves were wrapped in cling film and the stem was enclosed in a black plastic bag containing wet paper tissue. After 30 min of equilibration, the xylem water potential (Ψ_{xyl}) was measured. Stem segments were obtained from branches and progressively re-cut under water to the desired length of 5–10 cm. About 1 cm of bark was removed at both ends, and samples were connected to an hydraulic apparatus (Xyl'Em; Bronkhorst France S.A.S., Montigny-Les-Cormeilles, France). The measurement solution was a 10 mM KCl solution (filtered at 0.2 μm) in degassed mineral water (Nardini et al. 2007). Native stem hydraulic conductance (k_i) was initially measured under low water pressure ($P = 7$ kPa). Samples were then flushed at $P = 0.2$ MPa for 10 min to remove embolism and k was re-measured at low pressure to get maximum stem hydraulic conductance (k_{max}). The percent loss of stem hydraulic conductivity (PLC) was calculated as:

$$PLC = 100 \times [1 - (k_i/k_{max})]$$

One vulnerability curve (VC, sigmoidal with four parameters) for each species and in each site was generated by plotting all PLC values vs the corresponding Ψ_{xyl}, and the reference value Ψ_{50} (xylem water potential at 50% loss of conductance) was calculated.

Values of k_{max} were also used to calculate stem specific hydraulic conductivity (K_s) for each species and site as:

$$K_s = (k_{max} \times l)/A_x$$

where l is sample length and A_x is the transverse xylem area as calculated on the basis of xylem diameter measured using a digital calliper immediately after hydraulic measurements.

Finally, the safety margin (SM) experienced by the two species in the different sites was calculated as:

$$SM = \Psi_{min} - \Psi_{50}$$

Statistical analysis

After checking for data normality and homogeneity of variances, pairwise comparisons between means of each functional trait measured in the two study species were performed using a two-tailed Student's t-test where, for each couple of normally distributed populations, the null hypothesis that the means are equal was verified. This analysis was run through 't.test' function in 'stats' package for R software. Each functional trait was treated as a response variable, while species were treated as explanatory variables.

Two-way parametric ANOVA analysis was run to test differences between functional traits values of the study species through 'aov' function, in 'stats' package for R software. Each functional trait was treated as a response variable, while species and site were treated as explanatory variables. After checking for data normality and homogeneity of variances, post-hoc Tukey's Honestly Significant Differences comparisons were run through 'TukeyHSD' function in 'stats' package for R software when the main terms and their interaction in the ANOVA model resulted significant. Vulnerability curves were fitted through 'fitplcs' function in 'fit-PLC' package for R software and Ψ_{50} values and confidence intervals were calculated for each vulnerability curve. The Ψ_{50} value of a single vulnerability curve was considered different from the others if its confidence intervals did not overlap with confidence intervals calculated from the other vulnerability curves.

To summarize and visually describe the differences among traits of individuals of the two species in the two study sites, a Principal Component Analysis (PCA, R mode) was run through 'princomp' function in 'stats' package for R software. Before processing data, traits values were standardized (mean = 0; standard deviation = 1).

Results

Air temperature at the time of measurements ranged between 25.7 ± 0.5 and 29.4 ± 1.2 °C in the S and L site, respectively. Relative humidity was similar in the two sites ($41.9 \pm 2.1\%$ in L and $41.5 \pm 3.1\%$ in S), while marked differences were recorded in terms of PPFD, ranging from 21 ± 6 μmol m^{-2} s^{-1} in S to 1386 ± 249 μmol m^{-2} s^{-1} in L.

The mean values for all traits measured in Aa and Fo in the two study sites, and the relative standard deviations are summarized in Table 2 (data aggregated by species and site) and in

Table 2. Mean values ± standard deviation of functional traits measured in *A. altissima* and *F. ornus* in the site with high irradiance (L) and in shaded site (S). Different letters indicate significant differences between groups ($P < 0.05$).

	A. altissima		*F. ornus*	
	L	S	L	S
g_L, mmol m^{-2} s^{-1}	443.4 ± 76.6 a	219.3 ± 98.6 b	514.5 ± 177.3 a	234.1 ± 38.9 b
E_L, mmol m^{-2} s^{-1}	8.1 ± 1.9 a	2.7 ± 1.0 b	10.5 ± 4.4 a	3.0 ± 0.7 b
Ψ_{pd}, MPa	−0.5 ± 0.1 a	−0.5 ± 0.1 a	−0.4 ± 0.1 a	−0.3 ± 0.03 b
Ψ_{min}, MPa	−1.1 ± 0.1 a	−1.0 ± 0.2 a	−1.8 ± 0.3 b	−1.3 ± 0.2 a
π_O, MPa	−1.5 ± 0.3 a	−1.4 ± 0.3 a	−2.2 ± 0.2 b	−1.9 ± 0.8 a
Ψ_{tlp}, MPa	−1.4 ± 0.1 a	−1.1 ± 0.1 b	−1.9 ± 0.1 c	−1.5 ± 0.4 a
K_s, kg m^{-1} s^{-1} MPa^{-1}	8.0 ± 2.4 a	8.0 ± 3.0 a	1.6 ± 0.9 b	1.6 ± 0.6 b
k_{plant}, mmol m^{-2} s^{-1} MPa^{-1}	15.4 ± 6.0 a	5.5 ± 1.4 b	7.5 ± 2.1 b	3.2 ± 0.7 b
Ψ_{50}, MPa	−1.1	−1.3	−3.3	−3.0
SM, MPa	−0.03 ± 0.1 a	0.3 ± 0.2 a	1.5 ± 0.3 b	1.9 ± 0.2 b
WD, g cm^{-3}	0.5 ± 0.05 a	0.4 ± 0.1 a	0.7 ± 0.1 b	0.6 ± 0.1 b
C_{wood}, kg MPa^{-1} m^{-3}	66.1 ± 9.3 a	58.3 ± 8.8 a	21.5 ± 5.5 b	31.9 ± 12.5 b
LDMC, mg g^{-1}	411.9 ± 23.1 a	230.6 ± 5.2 b	408.8 ± 31.6 a	395.6 ± 12.7 a
SLA, mm^2 mg^{-1}	14.0 ± 3.3 a	37.0 ± 7.0 b	11.0 ± 2.4 a	16.8 ± 4.1 a
VLA$_{maj}$, mm^2 mm^{-1}	0.3 ± 0.02 a	0.3 ± 0.1 a	0.3 ± 0.1 a	0.2 ± 0.1 a
VLA$_{min}$, mm^2 mm^{-1}	12.5 ± 0.9 a	12.2 ± 1.9 a	8.8 ± 0.8 b	6.8 ± 1.2 b
C:N	23.8 ± 3.2 a	13.8 ± 3.2 b	29.7 ± 1.3 c	22.1 ± 1.3 a
C, %	47.2 ± 1.0 a	46.9 ± 0.7 a	47.8 ± 0.7 a	47.3 ± 0.9 a
N, %	2.0 ± 0.3 a	3.5 ± 0.8 b	1.6 ± 0.1 a	2.1 ± 0.1 a
$\delta^{13}C$, ‰	−27.7 ± 0.5 a	−29.4 ± 1.1 b	−27.6 ± 0.8 a	−29.1 ± 1.2 ab

Table S1 available as Supplementary Data at *Tree Physiology* Online (data aggregated by species). Individuals of both species had higher g_L and E_L in L site compared with the S one, with no differences between species (Figure 1). In particular, g_L was almost double in leaves under high irradiance compared with those in the shade, and these differences translated into an even larger increase of E_L (Figure 1) due to higher air temperatures in the L site than in S one.

Despite similar leaf-level rates of water loss, the water status of the two species was different. In fact, Ψ_{min} values measured in L site were significantly higher (less negative) in Aa than in Fo, while no inter-specific difference was recorded in S site (Figure 2). Ψ_{pd} values varied within a very narrow range and averaged −0.4 MPa (Figure 2). The water potential at turgor loss point (Ψ_{tlp}) changed accordingly to different light regimes (Figure 2), with significant lower values in L site compared with S site in both species. However, in both sites Fo had lower Ψ_{tlp} values (−2.4 MPa in L site and −1.9 MPa in S site) compared with Aa (−1.8 MPa in L site and −1.5 MPa in S site). These differences in Ψ_{tlp} were similar to those recorded for osmotic potential that in both light regimes was lower in Fo than in Aa (Figure 2).

Values of both K_s and k_{plant} were higher in Aa compared with Fo, especially in L site where K_s and k_{plant} were respectively fourfold and twofold higher in Aa than in Fo (Figure 3). Values of Ψ_{50} calculated from vulnerability curves of each species (Figure 4) did not differ between L and S sites, but were different in the two species. Fo had higher resistance to drought stress than Aa, with Ψ_{50} averaging −3.2 MPa and −1.2 MPa,

respectively. The safety margin against embolism formation experienced at midday was significantly lower in Aa where it was close to 0, than in Fo where it was very large and ranged between 1.5 and 1.9 MPa (Table 2, Figure 5).

The cost associated with the production of tissues devoted to water transport was lower in Aa than in Fo, as WD was ~0.5 g cm^{-3} in the former species compared with 0.7 g cm^{-3} in the latter (Figure 5). Differences between species in terms of WD apparently translated into differences in C_{wood}, which was higher in Aa than in Fo, with no significant differences between sites (Figure 5). Also leaf structural costs were different between species and sites. In fact, Aa had higher SLA values in the S site than in the L one, while Fo had similar values in both sites. Notably, in the S site the SLA of Aa was about double that of Fo. VLA$_{maj}$ did not change significantly between species and sites, while VLA$_{min}$ was significantly higher in Aa compared with Fo, again with no difference between sites (Figure 6).

Nutrient concentration varied according to the sites. Specifically, in both species C:N was higher in the L site than in the S site (Figure 7). Moreover, C:N was higher in Fo than in Aa. These differences mostly derived from variation in N content, as C content was rather constant at 47% across species and sites, while N was higher in Aa than Fo, and generally higher in S site compared with L site. Leaf carbon isotopic composition was similar in the two species, but values were significantly different in the two sites (Figure 7). In particular, $\delta^{13}C$ was significantly higher in the S site compared with the L site in both Aa and Fo.

The projection of individuals on axis 1 and 2 of the PCA (see Figure S1 available as Supplementary Data at *Tree Physiology*
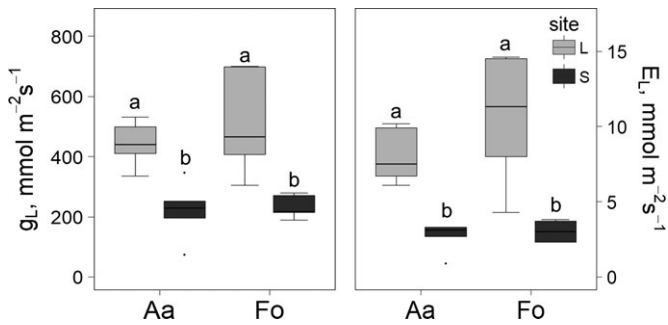
Figure 1. Median values, 25th and 75th percentiles of leaf conductance to water vapour (g_L) and leaf transpiration rates (E_L) measured in *A. altissima* (Aa) and in *F. ornus* (Fo) in L site (grey boxes) and in S site (dark grey boxes). Different letters indicate statistical significant differences among groups ($P < 0.05$).
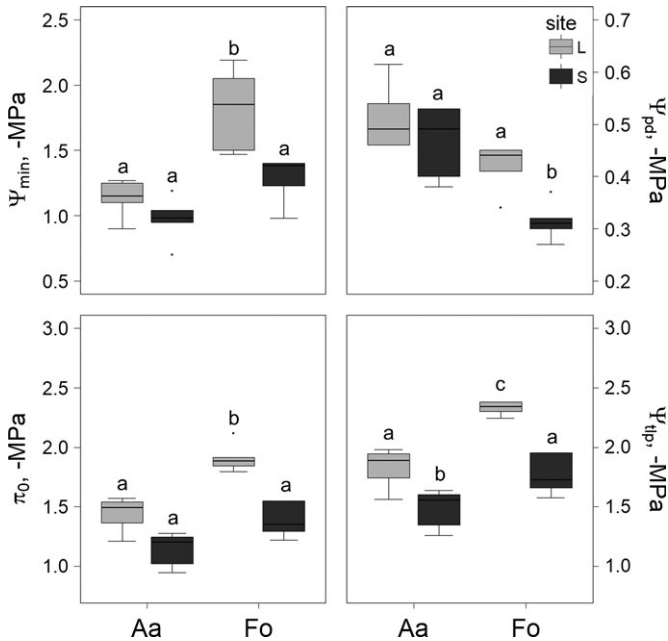

Figure 3. Median values, 25th and 75th percentiles of stem specific hydraulic conductivity (K_s), and whole-plant hydraulic conductance (k_{plant}) measured in *A. altissima* (Aa) and in *F. ornus* (Fo) in L site (grey boxes) and in S site (dark grey boxes). Different letters indicate statistical significant differences among groups ($P < 0.05$).

Figure 2. Median values, 25th and 75th percentiles of minimum leaf water potential (Ψ_{min}), pre-dawn leaf water potential (Ψ_{pd}), osmotic potential at full turgor (π_O) and water potential at turgor loss point (Ψ_{tlp}) measured in *A. altissima* (Aa) and in *F. ornus* (Fo) in L site (grey boxes) and in S site (dark grey boxes). Different letters indicate statistical significant differences among groups ($P < 0.05$).

Figure 4. Vulnerability curves reporting the relationship between percent loss of hydraulic conductivity (PLC) and xylem water potential (Ψ_{xyl}) measured in *A. altissima* and in *F. ornus* in L site (grey point and lines) and in S site (dark grey points and lines).

Online) confirmed a separation between the two species (axis 1, 47% of total explained variance) and between the two study sites with contrasting light availability (axis 2, 24% of total explained variance).

Discussion

Understanding which functional/mechanistic traits promote invasiveness of alien species is fundamental to understanding the mechanisms underlying plant invasions in different native vegetation types, and eventual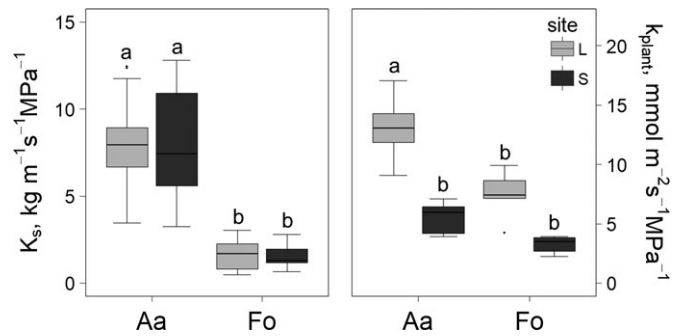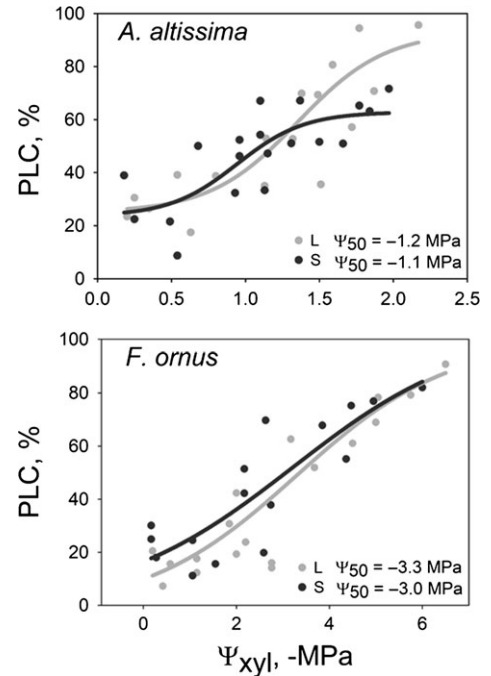ly predict the vulnerability of forests to alien tree invasions. In this study, key functional traits related to resource use and acquisition, with special reference to water use strategies, were compared in an alien species and a co-occurring native tree, growing in two sites with different light availability. We observed significant differences in some physiological and morphological traits, overall suggesting that the invasive potential of Aa is driven by a combination of reduced carbon costs for leaf and stem construction and high efficiency of water transport, translating into high productivity even though at the expense of hydraulic safety.
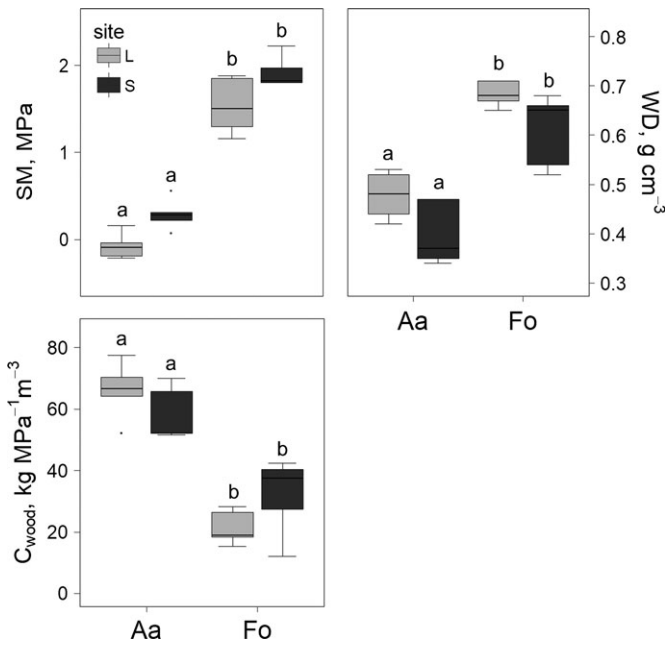
Figure 5. Median values, 25th and 75th percentiles of safety margin (SM), wood density (WD), and wood capacitance (C_{wood}) measured in *A. altissima* (Aa) and in *F. ornus* (Fo) in L site (grey boxes) and in S site (dark grey boxes). Different letters indicate statistical significant differences among groups ($P < 0.05$).
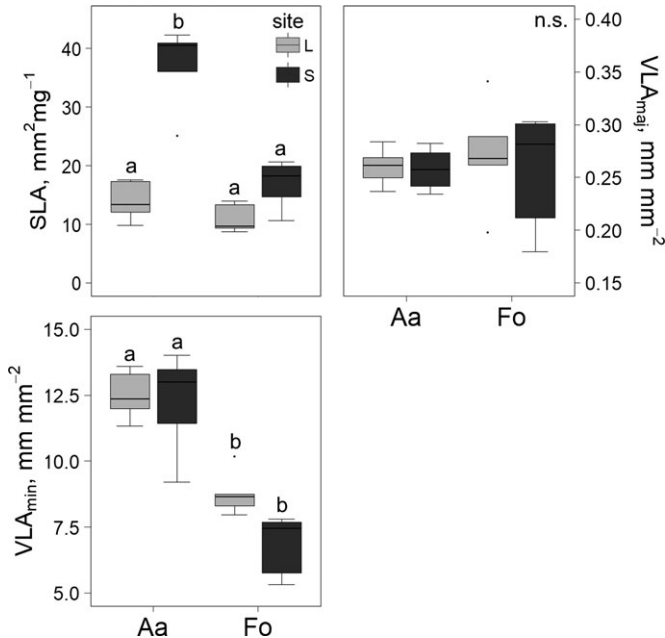

Figure 7. Median values, 25th and 75th percentiles of leaf C to N ratio (C:N), leaf C content (C), leaf N content (N) and leaf ^{13}C isotopic composition (δ^{13}C) measured in *A. altissima* (Aa) and in *F. ornus* (Fo) in L site (grey boxes) and in S site (dark grey boxes). Different letters indicate statistical significant differences among groups ($P < 0.05$), while n.s. indicates no significant differences ($P > 0.05$).
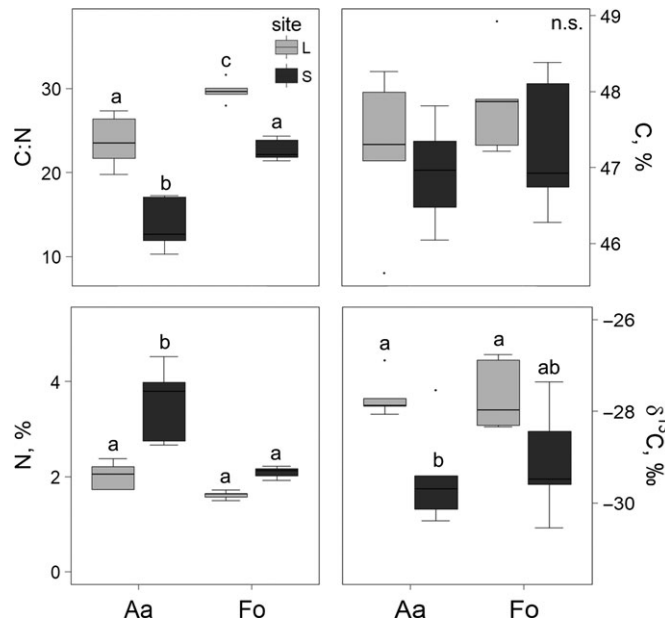

Figure 6. Median values, 25th and 75th percentiles of specific leaf area (SLA), major vein length per unit area (VLA_{maj}) and minor vein length per unit area (VLA_{min}) measured in *A. altissima* (Aa) and in *F. ornus* (Fo) in L site (grey boxes) and in S site (dark grey boxes). Different letters indicate statistical significant differences among groups ($P < 0.05$), while n.s. indicates no significant differences ($P > 0.05$).

Similar gas exchange rates but more favourable water status in invasive A. altissima compared with native F. ornus

The different incident light radiation in the two study sites had significant effects on gas exchange rates, as both species had lower g_L and E_L in the S site compared with the L one, but no differences were detected between the two species in this respect, as also confirmed by similar δ^{13}C values that represent a proxy for stomatal aperture integrated over longer time intervals than those typical of gas exchange measurements. Interestingly, despite similar leaf-level transpiration rates, plant water status was different in the two species. Aa had higher Ψ_{min} than Fo, with lower values in the L site for both species, in agreement with higher evaporative water losses under high irradiance. In general, Ψ_{min} is considered a proxy for the maximum water stress level experienced by an individual on a daily or seasonal scale. Different daily Ψ_{min} values in co-occurring species experiencing similar rates of water loss can be explained by three non-exclusive factors: (i) access to different water sources characterized by different soil water potential (Ehleringer and Dawson 1992); (ii) different hydraulic resistance in the soil-to-leaf water transport pathway (Sperry et al. 1998); and (iii) different hydraulic capacitance of stem and leaf tissues possibly buffering the water potential drop (McCulloh et al. 2012).

We did not estimate rooting depth of the study species. To the best of our knowledge, there are no data available about maximum rooting depth in Aa, although previous studies have

reported that lateral roots can spread to distances of ~27 m from the base of the plant, and down to 2 m below the soil surface (Kowarik and Säumel 2007). On the other hand, Fo was reported to undergo marked seasonal drop in pre-dawn water potential (Nardini et al. 2003), possibly suggesting prevalence of relatively shallow roots in this species. Thus, it is possible that Aa had access to more abundant water sources than Fo, and future analysis of xylem sap isotopic composition could provide useful information on rooting depth in these species (Nardini et al. 2016). However, it has to be noted that Ψ_{pd}, a commonly used proxy to estimate the water potential of soil volumes explored and exploited by the root system (Sellin 1999), was similar and quite high in both species. This would suggest that, regardless of eventual differences in rooting depth, the two species had no limitations in terms of water access and availability when measurements were performed.

Calculations of whole-plant hydraulic conductance (k_{plant}), as based on transpiration rates and soil-to-leaf water potential drop, revealed that Aa was about twofold more efficient in terms of root-to-leaf water transport capacity than Fo. This indirect estimate of k_{plant} was consistent with hydraulic measurements of stem specific hydraulic conductivity (K_s), which was fourfold higher in Aa than in Fo. Also, k_{plant} values were in agreement with recorded differences in terms of minor vein density (VLA_{min}), which was ~60% higher in Aa than in Fo. Vein density has been reported to correlate to leaf hydraulic conductance (Nardini et al. 2014b, Scoffoni et al. 2016). In turn, leaf hydraulic conductance is an important determinant of whole-plant hydraulic efficiency (Nardini 2001, Sack and Holbrook 2006). Hence, high vein density and high K_s of Aa probably contributed to an important extent to decrease resistances associated with long distance water transport, leading to moderate drop of leaf water potential even at relatively high transpiration, while similar water loss rates induced a much larger water potential drop in Fo. Finally, high wood capacitance recorded for Aa (~60 kg MPa^{-1} m^{-3} vs only 20–30 kg MPa^{-1} m^{-3} in Fo) was consistent with its lower wood density compared with Fo, and possibly contributed to buffer the water potential drop on a daily basis as previously suggested for other woody species (McCulloh et al. 2012, De Guzman et al. 2017, Epila et al. 2017).

The larger daily leaf water potential drop recorded in Fo compared with Aa did not necessarily translate into a major reduction of turgor pressure in the native tree, as also suggested by high midday values of g_L. This was apparently due to the fact that Fo had more negative values of π_O and Ψ_{tlp} than Aa. Indeed, values of $\Psi_{tlp} - \Psi_{min}$ were similar in the two species (~−0.6 MPa), suggesting that they experienced similar water stress levels during daytime. However, this was achieved by Fo only thanks to osmoregulation, which likely required important energetic inputs to accumulate and or synthesize solutes in mesophyll cells. Hence, a secondary advantage of high k_{plant} and C_{wood} of Aa was reduced costs for osmoregulation and turgor maintenance, so that it can be hypothesized that more carbohydrates remained

available for growth and biomass accumulation in this species than in the native one (Attia et al. 2015).

The safety–efficiency trade-off in invasive A. altissima compared with native F. ornus

Previous studies on different species' assemblages have suggested the existence of a trade-off between hydraulic efficiency and hydraulic safety (Tyree et al. 1994, Gleason et al. 2016). The current paradigm is that high hydraulic conductance derives from anatomical features, like wide xylem conduits and/or thin and permeable inter-conduit pit membranes, which increase the vulnerability of xylem to drought-induced embolism formation. We could detect this trend in our study species, as the high k_{plant} and K_s of Aa was coupled to high vulnerability to xylem embolism. Values of Ψ_{50} in Aa were ~−1.2 and −1.1 MPa in L and S site, respectively. Fo was significantly more resistant to embolism, with Ψ_{50} of ~−3.2 MPa consistent with low k_{plant} and K_s in this species. These differences were also in agreement with the higher wood density of Fo compared with Aa, as this trait has been reported to be correlated to embolism resistance (Nardini et al. 2013). Values of Ψ_{50} represent the intrinsic vulnerability of xylem to embolism. However, the actual risk of hydraulic failure to which different species are exposed does not depend simply on Ψ_{50}, but rather on the difference between Ψ_{50} and the actual Ψ_{min} reached by the species during the day or the whole growing season, i.e., on the so-called 'safety margin' (Choat et al. 2012). In Aa, the safety margin was close or slightly above 0 in L and S site, respectively. On the other hand, Fo maintained a very large safety margin of ~1.5–2.0 MPa. These findings suggest that Fo was not experiencing a significant risk of embolism development, consistent with a safe hydraulic construction, but likely requiring substantial carbon investment into wood construction as revealed by high WD. On the other hand, low WD in Aa probably significantly reduced carbon costs invested in wood formation, translating into high hydraulic efficiency per unit carbon invested, but also into a risky hydraulic strategy implying likelihood of embolism formation on a daily or seasonal scale. Interestingly, Aa has been reported to promptly close stomata under severe drought (Trifilò et al. 2004) and to rapidly recover from embolism following post-drought irrigation (Savi et al. 2016). In general terms, species with low WD and high C_{wood} have been reported to be more capable of embolism reversal than those with high WD and low C_{wood} (Trifilò et al. 2015). Hence, Aa and Fo might be an example of two species lying along the recently proposed trade-off between water use strategy, wood capacitance and embolism reversal ability (Klein et al. 2018, Nardini et al. 2018).

The wood and leaf economic spectra of A. altissima and F. ornus

Recently, Eller et al. (2018) depicted the possible trade-off between safety margin and tree growth rate, emerging from the

coordination between WD and Ψ_{50}. It was suggested that low construction costs (low wood density) in fast-growing species with narrow safety margins could allow these plants to achieve higher volumetric xylem production rates. As a consequence, the higher xylem volume available could allow fast-growing species like Aa to transport larger water volumes thus favouring expansion growth. Our results are overall consistent with this structural/physiological safety–efficiency framework, where higher efficiency in water transport in the invasive Aa implies higher hydraulic vulnerability but at lower wood construction costs, with potential benefits for carbon assimilation rates, growth and competition with native tree species. Hence, Aa and Fo would lie at the opposite extremes of this 'wood economic spectrum'.

Recent studies and meta-analyses (Leishman et al. 2007, van Kleunen et al. 2010) have reported that invasive species generally occupy a position along the global leaf economic spectrum that favours fast growth, with higher SLA, nitrogen content and photosynthetic capacity per unit leaf mass compared with native species. In this study, SLA was higher in Aa than in Fo, especially in the shaded site. This would suggest that Aa undergoes less carbon investment per unit leaf area construction, despite higher VLA_{min} (Nardini et al. 2012) and similar carbon content on a mass basis. Also, Aa had higher nitrogen concentration and lower C:N ratio than Fo in both L and S sites, suggesting high investments in the photosynthetic machinery in Aa (Gulías et al. 2003). However, these inter-specific differences did not translate into differences in terms of $\delta^{13}C$, consistent with similar levels of stomatal aperture in both Aa and Fo.

Functional plasticity and shade-tolerance of A. altissima and F. ornus

The magnitude of changes in different functional traits in response to light availability was overall larger in the invasive Aa compared with native Fo. In particular, Aa showed larger variations in terms of SLA, k_{plant}, C:N and N content between L and S sites, when compared with Fo. This would suggest that the functional plasticity of Aa is larger than that of Fo.

Interestingly, Aa is generally described as a shade-intolerant species, but the species has been recently reported to invade closed forest stands dominated by *Castanea sativa* L. in Southern Switzerland (Knüsel et al. 2017). The presence of large invasion spots in shaded habitats in our study area is in agreement with this report, and apparently consistent with the large functional plasticity of Aa. In particular, k_{plant} was much higher in the L site compared with S one, and this allowed Aa to exploit high light availability to maintain fully open stomata while buffering the diurnal water potential drop. Because K_s was similar in S and L sites, this increase in k_{plant} was likely due to changes at the root or leaf level, most likely in the extra-vascular water pathways that are known to be very dynamic and responsive to light conditions (Tyree et al. 2005). The large increase of

SLA recorded in Aa individuals growing in S site compared with L one is a typical response of shade-tolerant plants, where it helps to minimize leaf carbon construction costs while maximizing photosynthetic carbon gain per unit surface. The twofold increase of SLA in response to shade in Aa is in striking contrast to that of Fo, where SLA increased only by ~50%, suggesting that the native tree species is competitively disadvantaged even under low light conditions. Large phenotypic plasticity has been proposed as an important factor promoting invasiveness of alien plant species (Davidson et al. 2011) and this pattern is apparently confirmed by our data.

Conclusions

The comparison of several key functional and mechanistic traits of Aa, one of the most invasive species in Europe, and the native and outcompeted Fo, have revealed interesting patterns and overall suggest that a safety–efficiency trade-off provides a mechanistic framework to explain the invasive success of the alien tree. Traits related to leaf and wood construction costs and drought resistance significantly differed between the two species, with Fo sustaining higher structural costs than Aa. The lower resistance to drought stress of Aa was apparently counterbalanced by higher water transport efficiency, possibly requiring mechanisms to assure resilience to drought-induced hydraulic damage. Large phenotypic plasticity of Aa in response to light availability could also play a role in determining the invasive potential of this species. While we note that caution should be used when inferring species-specific drought resistance on the basis of physiological measurements performed over limited time intervals during the growing season, our data show that the measurement of mechanistic traits related to resource acquisition, with special reference to water-use strategies, could provide important novel insight into the mechanisms underlying the invasive nature of alien tree species in natural forest habitats.

References

Attia Z, Domec JC, Oren R, Way DA, Moshelion M (2015) Growth and physiological responses of isohydric and anisohydric poplars to drought. J Exp Bot 66:4373–4381.

Barotto AJ, Monteoliva S, Gyenge J, Martinez-Meier A, Fernandez ME (2018) Functional relationships between wood structure and vulnerability to xylem cavitation in races of Eucalyptus globulus differing in wood density. Tree Physiol 38:243–251.

Bartlett MK, Scoffoni C, Sack L (2012) The determinants of leaf turgor loss point and prediction of drought tolerance of species and biomes: a global meta-analysis. Ecol Lett 15:393–405.

Beikircher B, Mayr S (2016) Avoidance of harvesting and sampling artefacts in hydraulic analyses: a protocol tested on Malus domestica. Tree Physiol 36:797–803.

Binks O, Meir P, Rowland L et al. (2016) Plasticity in leaf-level water relations of tropical rainforest trees in response to experimental drought. New Phytol 211:477–488.

Bonan GB (2008) Forests and climate change: forcings, feedbacks, and the climate benefits of forests. Science 320:1444–1449.

Brodribb TJ (2009) Xylem hydraulic physiology: the functional backbone of terrestrial plant productivity. Plant Sci 177:245–251.

Brodribb TJ (2017) Progressing from 'functional' to mechanistic traits. New Phytol 215:9–11.

Bühler J, Rishmawi L, Pflugfelder D et al. (2015) phenoVein – a tool for leaf vein segmentation and analysis. Plant Physiol 169:2359–2370.

Caplan JS, Yeakley JA (2013) Functional morphology underlies performance differences among invasive and non-invasive ruderal Rubus species. Oecologia 173:363–374.

Caudullo G, Welk E, San-Miguel-Ayanz J (2017) Chorological maps for the main European woody species. Data Brief 12:662–666.

Cavaleri MA, Sack L (2010) Comparative water use of native and invasive plants at multiple scales: a global meta-analysis. Ecology 91:2705–2715.

Chiatante D, Di Iorio A, Sciandra S, Scippa GS, Mazzoleni S (2006) Effect of drought and fire on root development in Quercus pubescens Willd. and Fraxinus ornus L. seedlings. Environ Exp Bot 56:190–197.

Choat B, Jansen S, Brodribb TJ et al. (2012) Global convergence in the vulnerability of forests to drought. Nature 491:752–755.

Clayton JW, Fernando ES, Soltis PS, Soltis DE (2007) Molecular phylogeny of the Tree-of-Heaven family (Simaroubaceae) based on chloroplast and nuclear markers. Int J Plant Sci 168:1325–1339.

Constán-Nava S, Boneta A, Pastor E, Lledó MJ (2010) Long-term control of the invasive tree Ailanthus altissima: insights from Mediterranean protected forests. For Ecol Manage 260:1058–1064.

Corbett SL, Manchester SR (2004) Phytogeography and fossil history of Ailanthus (Simaroubaceae). Int J Plant Sci 165:671–690.

Crous CJ, Jacobs SM, Esler KJ (2012) Drought-tolerance of an invasive alien tree, Acacia mearnsii and two native competitors in fynbos riparian ecotones. Biol Invasions 14:619–631.

Davidson AM, Jennions M, Nicotra AB (2011) Do invasive species show higher phenotypic plasticity than native species and, if so, is it adaptive? A meta-analysis. Ecol Lett 14:419–431.

De Guzman ME, Santiago LS, Schnitzer SA, Álvarez-Cansino L (2017) Trade-offs between water transport capacity and drought resistance in neotropical canopy liana and tree species. Tree Physiol 37:1404–1414.

Ehleringer JR, Dawson TE (1992) Water uptake by plants: perspectives from stable isotope composition. Plant Cell Environ 15:1073–1082.

Eller CB, Barros FV, Bittencourt PRL, Rowland L, Mencuccini M, Oliveira RS (2018) Xylem hydraulic safety and construction costs determine tropical tree growth. Plant Cell Environ 41:548–562.

Epila J, De Baerdemaeker NJF, Vergeynst LL, Maes WH, Beeckman H, Steppe K (2017) Capacitive water release and internal leaf water relocation delay drought-induced cavitation in African Maesopsis eminii. Tree Physiol 37:481–490.

Funk JF, Standish RJ, Stock WD, Valladares F (2016) Plant functional traits of dominant native and invasive species in mediterranean-climate ecosystems. Ecology 97:75–83.

Gleason SM, Westoby M, Jansen S et al. (2016) Weak tradeoff between xylem safety and xylem-specific hydraulic efficiency across the world's woody plant species. New Phytol 209:123–136.

Gómez-Aparicio L, Canham CD (2008) Neighbourhood analyses of the allelopathic effects of the invasive tree Ailanthus altissima in temperate forests. J Ecol 96:447–458.

Gortan E, Nardini A, Gascó A, Salleo S (2009) The hydraulic conductance of Fraxinus ornus leaves is constrained by soil water availability and coordinated with gas exchange rates. Tree Physiol 29:529–539.

Gulías J, Flexas J, Mus M, Cifre J, Lefi E, Medrano H (2003) Relationship between maximum leaf photosynthesis, nitrogen content and specific leaf area in Balearic endemic and non-endemic Mediterranean species. Ann Bot 92:215–222.

Hember RA, Kurz WA, Coops NC (2017) Relationships between individual-tree mortality and water-balance variables indicate positive trends in water stress-induced tree mortality across North America. Glob Chang Biol 23:1691–1710.

Hughes FW (2005) Archimedes revisited: a faster, better, cheaper method of accurately measuring the volume of small objects. Phys Educ 40:468–474.

Kalapos T, Csontos P (2003) Variation in leaf structure and function of the Mediterranean tree Fraxinus ornus L. growing in ecologically contrasting habitats at the margin of its range. Plant Biosyst 137:73–82.

Klein T, Zeppel MJB, Anderegg WRL et al. (2018) Xylem embolism refilling and resilience against drought-induced mortality in woody plants: processes and trade-offs. Ecol Res. doi: 10.1007/s11284-018-1588-y.

Knüsel S, De Boni A, Conedera M, Schleppi P, Thormann JJ, Frehner M, Wunder J (2017) Shade tolerance of Ailanthus altissima revisited: novel insights from southern Switzerland. Biol Invasions 19:455–461.

Kowarik I, Säumel I (2007) Biological flora of Central Europe: Ailanthus altissima (Mill.) Swingle. Perspect Plant Ecol Evol Syst 8:207–237.

Lamarque LJ, Delzon S, Lortie CJ (2011) Tree invasions: a comparative test of the dominant hypotheses and functional traits. Biol Invasions 13:1969–1989.

Leishman MR, Haslehurst T, Ares A, Baruch Z (2007) Leaf trait relationships of native and invasive plants: community- and global-scale comparisons. New Phytol 176:635–643.

Luo Y, Yuan Y, Wang R, Liu J, Du N, Guo W (2016) Functional traits contributed to the superior performance of the exotic species Robinia pseudoacacia: a comparison with the native tree Sophora japonica. Tree Physiol 36:345–355.

Markesteijn L, Poorter L, Paz H, Sack L, Bongers F (2011) Ecological differentiation in xylem cavitation resistance is associated with stem and leaf structural traits. Plant Cell Environ 34:137–148.

McCulloh K, Johnson DJ, Meinzer FC, Voelker SL, Lachenbruch B, Domec JC (2012) Hydraulic architecture of two species differing in wood density: opposing strategies in co-occurring tropical pioneer trees. Plant Cell Environ 35:116–125.

Moser WK, Barnard EL, Billings RF et al. (2009) Impacts of nonnative invasive species on US forests and recommendations for policy and management. J For 107:320–327.

Nardini A (2001) Are sclerophylls and malacophylls hydraulically different? Biol Plant 44:239–245.

Nardini A (2002) Relations between efficiency of water transport and duration of leaf growth in some deciduous and evergreen trees. Trees 16:417–422.

Nardini A, Luglio J (2014) Leaf hydraulic capacity and drought vulnerability: possible trade-offs and correlations with climate across three major biomes. Funct Ecol 28:810–818.

Nardini A, Lo Gullo MA, Salleo S (1999) Competitive strategies for water availability in two Mediterranean *Quercus* species. Plant Cell Environ 22:109–116.

Nardini A, Salleo S, Trifilò P, Lo Gullo MA (2003) Water relations and hydraulic characteristics of three woody species co-occurring in the same habitat. Ann For Sci 60:297–305.

Nardini A, Gascó A, Trifilò P, Lo Gullo MA, Salleo S (2007) Ion-mediated enhancement of xylem hydraulic conductivity is not always suppressed by the presence of Ca^{2+} in the sap. J Exp Bot 58:2609–2615.

Nardini A, Pedà G, La Rocca N (2012) Trade-offs between leaf hydraulic capacity and drought vulnerability: morpho-anatomical bases, carbon costs and ecological consequences. New Phytol 196:788–798.

Nardini A, Battistuzzo M, Savi T (2013) Shoot desiccation and hydraulic failure in temperate woody angiosperms during an extreme summer drought. New Phytol 200:322–329.

Nardini A, Lo Gullo MA, Trifilò P, Salleo S (2014a) The challenge of the Mediterranean climate to plant hydraulics: responses and adaptations. Environ Exp Bot 103:68–79.

Nardini A, Õunapuu-Pikas E, Savi T (2014b) When smaller is better: leaf hydraulic conductance and drought vulnerability correlate to leaf size and venation density across four *Coffea arabica* genotypes. Funct Plant Biol 41:972–982.

Nardini A, Casolo V, Dal Borgo A et al. (2016) Rooting depth, water relations and non-structural carbohydrate dynamics in three woody angiosperms differentially affected by an extreme summer drought. Plant Cell Environ 39:618–627.

Nardini A, Savi T, Trifilò P, Lo Gullo MA (2018) Drought stress and the recovery from xylem embolism in woody plants. Prog Bot 79:197–231.

Neumann M, Mues V, Moreno A, Hasenauer H, Seidl R (2017) Climate variability drives recent tree mortality in Europe. Glob Chang Biol 23:4788–4797.

Nicotra AB, Atkin OK, Bonser SP et al. (2010) Plant phenotypic plasticity in a changing climate. Trends Plant Sci 15:684–692.

Oliveira MT, Souza GM, Pereira S, Oliveira DAS, Figueiredo-Lima KV, Arruda E, Santos MG (2017) Seasonal variability in physiological and anatomical traits contributes to invasion success of *Prosopis juliflora* in tropical dry forest. Tree Physiol 37:326–337.

Pejchar L, Mooney HA (2009) Invasive species, ecosystem services and human well-being. Trends Ecol Evol 24:497–504.

Petruzzellis F, Palandrani C, Savi T, Alberti R, Nardini A, Bacaro G (2017) Sampling intraspecific variability in leaf functional traits: practical suggestions to maximize collected information. Ecol Evol 7:11236–11245.

Poorter H, Niinemets U, Poorter L, Wright IJ, Villar R (2009) Causes and consequences of variation in leaf mass per area (LMA): a meta-analysis. New Phytol 182:565–588.

Pratt RB, Black RA (2006) Do invasive trees have a hydraulic advantage over native trees? Biol Invasions 8:1331–1341.

Pyšek P, Jarošík V, Hulme PE, Pergl J, Hejda M, Schaffner U, Vilá M (2012) A global assessment of invasive plant impacts on resident species, communities and ecosystems: the interaction of impact measures, invading species' traits and environment. Glob Chang Biol 18:1725–1737.

Richards CL, Bossdorf O, Muth NZ, Gurevitch J, Pigliucci M (2006) Jack of all trades, master of some? On the role of phenotypic plasticity in plant invasions. Ecol Lett 9:981–993.

Sack L, Holbook NM (2006) Leaf hydraulics. Ann Rev Plant Biol 57:361–381.

Savi T, Casolo V, Luglio J, Bertuzzi S, Trifilò P, Lo Gullo MA, Nardini A (2016) Species-specific reversal of stem xylem embolism after a prolonged drought correlates to endpoint concentration of soluble sugars. Plant Physiol Biochem 106:198–207.

Savi T, Love V, Dal Borgo A, Martellos S, Nardini A (2017) Morpho-anatomical and physiological traits in saplings of drought-tolerant Mediterranean woody species. Trees 31:1137–1148.

Schachtschneider K, February EC (2013) Impact of *Prosopis* invasion on a keystone tree species in the Kalahari Desert. Plant Ecol 214:597–605.

Scoffoni C, Chatelet DS, Pasquet-kok J, Rawls M, Donoghue MJ, Edwards EJ, Sack L (2016) Hydraulic basis for the evolution of photosynthetic productivity. Nat Plants 2:16072.

Sellin A (1999) Does pre-dawn water potential reflect conditions of equilibrium in plant and soil water status? Acta Oecol 20:51–59.

Sladonja B, Sušek M, Guillermic J (2015) Review on invasive tree of heaven (*Ailanthus altissima* (Mill.) Swingle) conflicting values: assessment of its ecosystem services and potential biological threat. Environ Manage 56:1009–10034.

Sperry JS, Adler FR, Campbell GS, Comstock JP (1998) Limitation of plant water use by rhizosphere and xylem conductance: results from a model. Plant Cell Environ 21:347–359.

Stratton LC, Goldstein G (2001) Carbon uptake, growth and resource-use efficiency in one invasive and six native Hawaiian dry forest tree species. Tree Physiol 21:1327–1334.

Trifilò P, Raimondo F, Nardini A, Lo Gullo MA, Salleo S (2004) Drought resistance of *Ailanthus altissima*: root hydraulics and water relations. Tree Physiol 24:107–114.

Trifilò P, Raimondo F, Lo Gullo MA, Barbera PM, Salleo S, Nardini A (2014) Relax and refill: xylem rehydration prior to hydraulic measurements favours embolism repair in stems and generates artificially low PLC values. Plant Cell Environ 37:2491–2499.

Trifilò P, Nardini A, Lo Gullo MA, Barbera PM, Savi T, Raimondo F (2015) Diurnal changes in embolism rate in nine dry forest trees: relationships with species-specific xylem vulnerability, hydraulic strategy and wood traits. Tree Physiol 35:694–705.

Tyree MT (2003) Hydraulic limits on tree performance: transpiration, carbon gain and growth of trees. Trees 17:95–100.

Tyree MT, Davis SD, Cochard H (1994) Biophysical perspectives of xylem evolution – is there a tradeoff of hydraulic efficiency for vulnerability to dysfunction? IAWA J 15:335–360.

Tyree MT, Nardini A, Salleo S, Sack L, El Omari B (2005) The dependence of leaf hydraulic conductance on irradiance during HPFM measurements: any role for stomatal response? J Exp Bot 56:737–744.

Urli M, Porté AJ, Cochard H, Guengant Y, Burlett R, Delzon S (2013) Xylem embolism threshold for catastrophic hydraulic failure in angiosperm trees. Tree Physiol 33:672–683.

van Kleunen M, Dawson W, Schlaepfer D, Jeschke JM, Fischer M (2010) Are invaders different? A conceptual framework of comparative approaches for assessing determinants of invasiveness. Ecol Lett 13:947–958.

Wright IJ, Reich PB, Westoby M et al. (2004) The worldwide leaf economics spectrum. Nature 428:821–827.

Yazaki K, Sano Y, Fujikawa S, Nakano T, Ishida A (2010) Response to dehydration and irrigation in invasive and native saplings: osmotic adjustment versus leaf shedding. Tree Physiol 30:597–607.

Zeballos SR, Giorgis MA, Cingolani AM, Cabido M, Whitworth-Hulse JI, Gurvich DE (2014) Do alien and native tree species from Central Argentina differ in their water transport strategy? Austral Ecol 39:984–991.

Zhu SD, Chen YJ, Fu PL, Cao KF (2017) Different hydraulic traits of woody plants from tropical forests with contrasting soil water availability. Tree Physiol 37:1469–1477.